

# Modeling the Radiance of the Moon for On-orbit Calibration

Thomas C. Stone, Hugh H. Kieffer, and Kris J. Becker

US Geological Survey, 2255 N. Gemini Drive, Flagstaff, AZ, 86001

## ABSTRACT

The RObotic Lunar Observatory (ROLO) project has developed radiometric models of the Moon for disk-integrated irradiance and spatially resolved radiance. Although the brightness of the Moon varies spatially and with complex dependencies upon illumination and viewing geometry, the surface photometric properties are extremely stable, and therefore potentially knowable to high accuracy. The ROLO project has acquired 5+ years of spatially resolved lunar images in 23 VNIR and 9 SWIR filter bands at phase angles up to 90°. These images are calibrated to exoatmospheric radiance using nightly stellar observations in a band-coupled extinction algorithm and a radiometric scale based upon observations of the star Vega. An effort is currently underway to establish an absolute scale with direct traceability to NIST radiometric standards. The ROLO radiance model performs linear fitting of the spatially resolved lunar image data on an individual pixel basis. The results are radiance images directly comparable to spacecraft observations of the Moon. Model-generated radiance images have been produced for the ASTER lunar view conducted on 14 April 2003. The radiance model is still experimental – simplified photometric functions have been used, and initial results show evidence of computational instabilities, particularly at the lunar poles. The ROLO lunar image dataset is unique and extensive and presents opportunities for development of novel approaches to lunar photometric modeling.

**Keywords:** On-orbit calibration, Moon, Radiance

## 1. INTRODUCTION

The Robotic Lunar Observatory (ROLO) project has established a facility for high-accuracy radiometric measurements of the Moon with the goal of utilizing the Moon for on-orbit radiometric calibration of spacecraft instruments.<sup>1</sup> Although the reflectance properties of the lunar surface are extremely stable,<sup>2</sup> the complex dependence on illumination and viewing angles necessitates a use of a photometric model to predict the lunar radiance (or reflectance) for a given observation geometry. The technique and practical methods of lunar calibration have been developed by ROLO primarily in the context of a model for the disk-integrated lunar irradiance<sup>3–6</sup>; comparisons have been made of spacecraft-measured lunar irradiance against ROLO model predictions for several instruments.<sup>7,8</sup> For imaging instruments whose optical configurations do not permit capture of the entire Moon in a practical manner, a spatially resolved radiance model is required. The computational tools have been developed for fitting the extensive ROLO lunar image database on an individual pixel basis, and ROLO has demonstrated the capability to produce radiance images of the Moon congruent to spacecraft observations. The current status of this work is spatially co-registering the model results to spacecraft imagery for direct radiance comparisons.

## 2. ROLO LUNAR CALIBRATION

Fundamental to ROLO lunar calibration is a set of absolute radiometric measurements of the Moon acquired with a ground-based telescope system. These images, processed to exoatmospheric radiance, provide the input data to photometric models designed around the primary geometric variables of illumination and viewing. Spacecraft measurements of the Moon are compared against model results generated for the specific geometry of a spacecraft observation. A protocol has been established for interfacing with spacecraft teams in order to accommodate the participation of an increasing number of instruments in ROLO lunar calibration.

---

Further author information: (Send correspondence to T.C.S.)  
e-mail: tstone@usgs.gov, telephone: 928-556-7381  
H.H.K.: e-mail: hkieffer@usgs.gov; K.J.B. e-mail: kbecker@usgs.gov

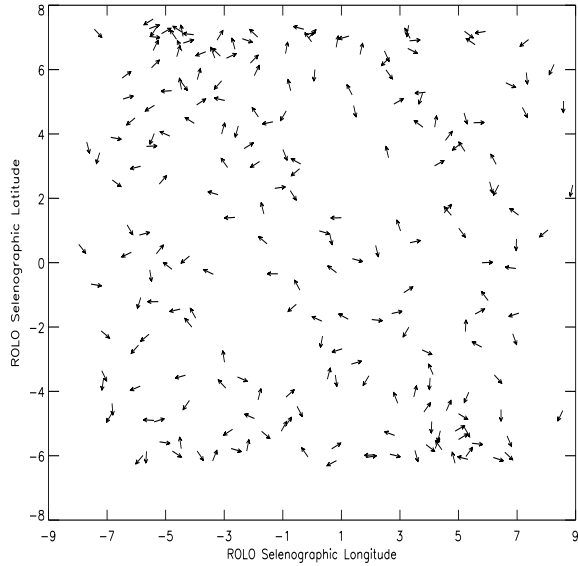


**Figure 1.** Libration coverage with phase information for the current processed ROLO database. Phase angle is indicated by the direction of the arrows;  $0^\circ$  is shown as vertical up. Each data point is an average for one observing night.

## 2.1. Lunar Image Database

The ROLO facility is located on-site at the USGS field center in Flagstaff, Arizona [lat.  $32^\circ 12' 52.9''$ N, lon.  $111^\circ 38' 5.0''$ W, alt. 2148 m]. Tandem, nearly identical telescopes view the Moon every clear night from lunar first quarter to last quarter. The two cameras cover the Visible/Near-IR (VNIR) wavelength region in 23 bands from 350 to 950 nm and Shortwave-IR (SWIR) wavelengths in 9 bands from 950 to 2350 nm. Spatial resolution is 4.08 arcseconds in VNIR (nominal Moon diameter  $\sim$ 500 pixels) and 8.24 arcsec in the SWIR. As part of the post-acquisition processing, images from both cameras are projected onto a  $576 \times 576$  pixel grid in a modified Lambert Equal-Area Azimuthal projection which covers all points on the Moon visible from Flagstaff, referred to here as the “ALEX” projection. The majority of nightly observation time is dedicated to imaging a subset of about 170 standard stars for use in determining atmospheric extinction corrections and also as a supplementary measure of the telescope systems’ absolute responsivity.

The ROLO telescope systems have been in operation in their current configuration since January 1998 and have acquired over 85 000 individual images of the Moon and  $\sim 10^6$  images of stars. The goal is to cover as wide a range of phase and libration angles as practical – the original project concept anticipated that 4.5 years, about one quarter of the lunar libration cycle, would suffice.<sup>1</sup> Figure 1 shows the phase+libration coverage of the current ROLO observational database, with each arrow representing one night’s observations. The coverage in selenographic latitude/longitude space is substantial; however, for a given small range of phase angle (typical of a spacecraft lunar observing program) the libration coverage is quite limited. This becomes apparent by isolating parallel arrows in the figure.

For use in photometric models, the ROLO lunar images are calibrated to exoatmospheric radiance and summed over the entire observed lunar disk, regardless of illuminated fraction. Corrections to above-the-atmosphere are generated from the nightly stellar observations by a time-dependent extinction model which fits all the ROLO bands simultaneously and allows the atmospheric absorbing species to vary in concentration through the night. The absolute radiometric scale currently is derived from ROLO measurements of the star Vega. The spectral irradiance of Vega is derived from a synthetic stellar spectrum<sup>9</sup> scaled to astronomical abso-

lute photon flux measurements.<sup>10, 11</sup> This spectrum is then convolved with the ROLO system spectral response in each band. Recent comparisons of the ROLO system response to known radiance calibration sources have shown that this Vega-based radiance scale is somewhat uncertain. A dedicated effort is currently underway to determine the ROLO absolute scale with traceability to NIST radiometric standards.

The coefficients for radiance calibration, atmospheric correction, and the lunar disk integrations for each image frame are tabulated in the headers of the image-cube files as part of the standard data processing. At the end of each major data reduction run, these and other ancillary data, e.g. ephemeris and observation geometry parameters (80 parameters total per image frame), are collected into a contiguous auxiliary parameter file which covers the entire dataset.

## 2.2. Lunar Irradiance Model

Because the reflectance of the Moon exhibits a strong dependence on illumination and viewing geometry, space-craft observations cannot be compared directly to ROLO imagery (other than fortuitous coincidence). Rather, the ROLO observational data have been used to develop a lunar reflectance model based on the fundamental geometric variables (incidence, emission and phase angles), which can be interrogated for a particular space-craft observation geometry. To date, all applications of ROLO lunar calibration to spacecraft instruments have involved comparisons of disk-integrated lunar irradiance.

The approach of ROLO irradiance modeling is strictly empirical – virtually all published lunar photometric models have been tried,<sup>12–17</sup> including full Hapke theory<sup>18</sup>; none were found to fit the ROLO observations to the accuracy potential of the data. The analytic form of the irradiance model has been developed with the goal of fitting the observational data to the extent that no correlations exist within the fit residuals. The quantity fitted is lunar reflectance, corrected to standard distances of 1 AU for Sun–Moon and 384 400 km for Moon–Observer. Disk-integrated irradiance  $I_k$  is converted to reflectance  $A_k$  by the relation:

$$I_k = A_k \cdot \Omega_M \cdot E_{\lambda_S k} / \pi \quad (1)$$

where  $E_{\lambda_S k}$  is the solar irradiance at effective wavelength  $\lambda_S$  for a band  $k$ ;  $\Omega_M = 6.4236 \times 10^{-5}$  sr. This conversion involves a model for solar spectral irradiance. Comparisons of solar models currently in use show significant differences at some wavelengths, which may lead to uncertainties in the lunar irradiance measured by spacecraft instruments using different solar models. For ROLO modeling work, the WCRP solar irradiance data<sup>19</sup> is used.

The irradiance model form is an expression in the natural log of reflectance as a function of the primary geometric variables:

$$\ln A_k = \sum_{i=0}^3 a_{ik} g^i + \sum_{j=1}^3 b_{jk} \Phi^{2j-1} + c_1 \theta + c_2 \phi + c_3 \Phi \theta + c_4 \Phi \phi + d_{1k} e^{-g/p_1} + d_{2k} e^{-g/p_2} + d_{3k} \cos((g - p_3)/p_4) \quad (2)$$

where  $g$  is the absolute phase angle,  $\theta$  and  $\phi$  are the selenographic latitude and longitude of the observer, and  $\Phi$  is the selenographic longitude of the Sun. Detailed descriptions of the terms in Equation 2, along with discussions of the internal consistency of the model and applications to spacecraft instruments, can be found in previous publications.<sup>3, 7</sup>

The lunar reflectance produced by the ROLO irradiance model exhibits some modest spectral excursions, whereas spectrophotometric studies of the Moon have shown the actual reflectance features are broad and shallow.<sup>20–23</sup> The irregular ROLO results may stem from the solar spectral model used or may be an effect of the absolute calibration of the ROLO observational systems which is derived from measurements of the star Vega. Currently the radiometric scale of the ROLO systems is somewhat uncertain; a dedicated effort is in progress to establish traceability of the absolute scale to NIST radiometric standards. The current level of precision being demonstrated by ROLO irradiance modeling<sup>7</sup> suggests the potential for lunar calibration to achieve a sub-percent level of absolute accuracy – reaching this goal may ultimately require above-the-atmosphere measurements with direct traceability to international standards.

### **2.3. Spacecraft Lunar Observations**

Lunar calibration generally requires normally nadir-viewing satellites to execute an attitude maneuver in order to observe the Moon. This can be a pure pitch rotation or a combination pitch and roll, which eases the geometric viewing constraints somewhat. SeaWiFS has made 70 lunar observations beginning November 1997. The attitude maneuver is pitch-only, however the SeaWiFS instrument can be biased  $20^\circ$  to either side of nadir to reduce the effects of ocean glint; this capability is utilized for lunar image acquisition. The EO-1 spacecraft has executed pitch-and-roll maneuvers to capture the Moon in the ALI and Hyperion instruments on alternate months since February 2001. On 14 April 2003 the Terra spacecraft executed a calibration maneuver which allowed all of its imaging instruments to view the Moon, including the ASTER stereo telescope and all nine MISR cameras.

Attitude maneuvers typically start when the spacecraft passes into the Earth's shadow and are completed before the spacecraft re-emerges into sunlight. For the Terra maneuver, the normally nadir-locked pitch rate is reversed and held constant to slew past the Moon at an angular velocity about  $4\frac{1}{2}$  times slower than the normal nadir viewing rate, resulting in an oversampling factor of this amount. The entire maneuver requires roughly 30 minutes to execute.

In support of the Terra Deep Space Calibration Maneuvers with lunar views, ROLO has developed capabilities to predict Moon observation opportunities for pitch-only maneuvers based upon precise planetary ephemeris and satellite orbital element information. Computations of satellite acceleration and rotation rates can be included to produce lunar image acquisition times for normally nadir-pointed instruments.

### **2.4. Spacecraft Team Interaction**

To facilitate the increasing number of spacecraft instrument teams desiring lunar calibration comparisons, ROLO has developed a protocol for information exchange [<http://www.moon-cal.org> → Spacecraft Calibration → Information Exchange Items]. The spacecraft team provides to ROLO their instrument Relative Spectral Response and the cross-track resolution and field of regard of the optical system; then for each observation provides the UTC and spacecraft location in J2000 coordinates, the down-track size of the Moon in the acquired image (equal to the oversampling factor), and the disk-integrated irradiance as determined from the normal instrument calibration coefficients. ROLO calculates the positions of the Sun and Moon at the time of the observation, applies corrections to standard distances, interrogates the lunar reflectance model for the observation geometry, converts the predicted reflectance to irradiance at the spacecraft band effective wavelengths, and provides to the spacecraft team the discrepancy between the ROLO predictions and the spacecraft measured irradiance.

## **3. LUNAR RADIANCE MODEL**

To accommodate high-resolution instruments which cannot capture the entire Moon in a practical manner, and to properly account for spacecraft lunar images which may be clipped on one side, ROLO has developed a fully spatially resolved lunar radiance model. The computational complexity of fitting thousands of input images at single-pixel resolution is substantial, requiring novel programming techniques to overcome the practical limitations of e.g. machine memory. Although the ROLO radiance model is still under development, comparison radiance images have been generated for the ASTER lunar view acquired from the April 2003 Terra Deep Space Calibration Maneuver.

### **3.1. Data Selection and Pre-Processing**

Familiarity with the ROLO dataset gained from the irradiance modeling effort has provided data selection criteria for the preliminary radiance model runs – selected data are constrained to complete 32-band series and a list of nights identified as having extremely favorable observing conditions. This process leaves about 1150 images in each band. Further selection is performed within the fitting process on a per-pixel basis: outlier points deviating  $> 3\sigma$  are removed and the fit is iterated. As analysis of these rejection incidences proceeds, the constraints on input data selection will be supplanted.

For the initial radiance model runs, individual pixels of the ALEX-projected lunar images are fitted independently. To facilitate machine loading of pixel values from the entire dataset at once, a precursory transposing of the  $\sim 100$ -Gbyte ALEX dataset was required. This process involves subsampling each image and concatenating

the span of the archive, currently 67505 processed images. Based on finding a manageable size for the transposed files and to accommodate the addition of more recent data acquisitions, the subsample size chosen was 3 image lines by the 576-pixel full image width. Each of the resulting “bricks” is currently about 466Mb.

The individual ALEX image pixels are calibrated and corrected to exoatmospheric radiance at standard distances (Sun–Moon = 1 AU, Moon–Observer = 384 400 km), then converted to reflectance using Equation 1 with  $I_k$  representing the radiance of a pixel. The incidence, emission and phase angles for each pixel location are generated from the ALEX cartographic system and the selenographic directions to the Sun and the ROLO telescope.

### 3.2. Radiance Model Form

Since a spatially resolved photometric description of the Moon must account for the variation in incidence and emission angles over the illuminated sphere at a given phase angle, the geometrically simplified form of the irradiance model cannot be employed in this context. In addition, the computational resources needed to process  $\sim 200\,000$  individual pixels places practical limitations on the use of non-linear methods and empirical development of the model form based on inspection of fit residuals.

The initial radiance model runs have employed linear solution methods with basis functions adapted from bidirectional reflectance theory.<sup>18</sup> This choice of methods leaves no tractable provision for the non-linear photometric properties of the Moon such as the enhanced backscatter observed at low phase angles – the lunar “opposition effect”. Consequently the reflectance values input to the model  $A'_k$  are pre-conditioned using the two opposition effect terms of Eqn. 2 (nominally representing shadow hiding and coherent backscatter). For each image pixel reflectance  $A_k$ :

$$A'_k = \frac{A_k}{P_k(g)} \quad \text{where} \quad \ln P_k(g) = d_{1k} e^{-g/p_1} + d_{2k} e^{g/p_2} \quad (3)$$

The values of the coefficients  $d_{1k}$ ,  $p_1$ ,  $d_{2k}$  and  $p_2$  are taken from the irradiance model fit results for the band  $k$  of interest.

The analytic form currently used is an adaptation of the Lunar-Lambert photometric function of Refs. 24 and 25:

$$A'_k(g, \mu_0, \mu) = 2 L(g) \frac{\mu_0}{\mu + \mu_0} + [1 - L(g)] \mu_0 \quad \text{with} \quad L(g) = 1 + \sum_{i=1}^3 a_i g^i \quad (4)$$

where  $g$  is the phase angle,  $\mu_0 = \cos(\text{incidence angle})$ , and  $\mu = \cos(\text{emission angle})$ . The method of solution is singular value decomposition, although lower/upper triangular decomposition is an alternate option. SVD error evaluations are available for each fit coefficient  $a_i$  for each pixel. The relative SVD error values averaged over all pixels is on the order of  $10^{-3}$  for each band, however this quantity is representative of the precision of the solution and is not considered a reliable measure of the overall accuracy of the model.

### 3.3. Preliminary Results

The end-product of the ROLO radiance model is a radiometrically and geometrically correct image of the Moon corresponding to a spacecraft instrument observation. This is accomplished in two steps: calculations of the solar and lunar ephemeris for the time and location of the spacecraft observation are used to evaluate the illumination and phase angle geometry, and an appropriate ALEX-projected image is generated; this image is then re-projected to the perspective of the spacecraft view.

As a test case, the Terra/ASTER lunar view has been used to exercise the radiance image generation routines. ASTER viewed the Moon at approximately 22:10 UTC on 14 April 2003, at  $-27.7^\circ$  phase angle (negative phase angles are used by ROLO to distinguish lunar phases before full moon). Figure 2 shows the ASTER band 1 (550 nm) image, aspect-corrected for the oversampling rate to give a circular lunar disk.

Figure 3 is the radiance model-generated image in the ROLO 550 nm band, projected to the perspective of the ASTER lunar view. The predictions of bright features and albedo variations among mare and highlands generally appear quite satisfactory, although there are some anomalous effects at the latitude extremes and near



**Figure 2.** ASTER image of the Moon, acquired 14 April 2003, band 1 (550 nm). The Level-0B1 image has been corrected for the oversampling factor of 4.58 in the down-track direction. Lunar North is approximately 11 o'clock in this figure.

the eastern limb. The bright bands highlighting the dark limb and at the edge of the ALEX projection are artifacts of the model solution, probably due to under-representation in the input data at these points, although checks for this condition are built into the algorithm. The image is somewhat blurred, possibly indicative of small pixel registration errors in the input ALEX images. At present, co-registration of this model image to the ASTER image to allow direct comparison of the lunar radiance is work in progress.

### 3.4. Discussion

Although the capability to generate spatially resolved lunar radiance images at spacecraft perspectives has been demonstrated, it must be emphasized that ROLO efforts in photometric modeling for this application are still in preliminary development stages. At present, the model form is linear in the geometric variables of incidence, emission and phase angles, which places undue restrictions on the photometric description being modeled. Methods which adequately treat the physical properties of lunar reflectance are clearly needed.

The software developed for the ROLO radiance model is a modular, object-oriented system, readily adaptable to alternative model forms, criteria for input data selection, and choice of solution methods. This allows basis equations for fitting data to rapidly be designed within a plug-in module framework which is dynamically implemented at runtime. The same program module gets used for function evaluation with the generated fit coefficients for a specified illumination/observation geometry. This programming technique serves to insulate the task of designing photometric descriptions from the complexities of computational resource management for such a large dataset.

Additional ROLO project efforts involve exploring alternative approaches to radiance modeling which fully exploit the extensive spatially resolved lunar radiometric dataset acquired by the ROLO observational program. For example, a principal component analysis in the primary geometric variables has been initiated.



**Figure 3.** ROLO model radiance image, projected to the perspective of the ASTER lunar view.

#### 4. CONCLUSIONS

The ROLO program for on-orbit calibration has acquired an extensive set of spatially resolved radiometric measurements of the Moon, from which the capability has been developed for generating lunar radiance images corresponding to spacecraft observations. The preliminary version of this radiance model includes a number of adaptations from ROLO lunar irradiance modeling. The programming framework of the ROLO radiance model allows for rapid development and testing of model forms for describing lunar photometric properties.

The ROLO observational data provides coverage in phase and libration angles at spatial and spectral resolution comparable to no known dataset. This collection offers significant new opportunities for advancement of the study of lunar photometric properties. Current ROLO modeling efforts are examining alternative approaches, the use of non-linear methods, and testing of physical models, e.g. the shadow hiding explanation of the opposition effect.

#### ACKNOWLEDGMENTS

The authors thank Hiroshi Watanabe and Akira Iwasaki for providing the ASTER lunar data. The ROLO project is supported by Goddard Space Flight Center as part of NASA's Earth System Enterprise under contract S-41359-F.

#### REFERENCES

1. H. H. Kieffer and R. L. Wildey, "Establishing the Moon as a spectral radiance standard," *J. of Atmospheric and Oceanic Technology* **13**(2), pp. 360–375, 1996.
2. H. H. Kieffer, "Photometric stability of the lunar surface," *Icarus* **130**, pp. 323–327, 1997.

3. T. C. Stone and H. H. Kieffer, "Absolute irradiance of the Moon for on-orbit calibration," *Proc. SPIE* **4814**, pp. 211–221, 2002.
4. T. C. Stone, H. H. Kieffer, and J. M. Anderson, "Status of use of lunar irradiance for on-orbit calibration," *Proc. SPIE* **4483**, pp. 165–175, 2002.
5. J. M. Anderson, H. Kieffer, and K. Becker, "Modeling the brightness of the Moon over 350-2500 nm for spacecraft calibrations," *Proc. SPIE* **4169**, pp. 248–259, 2000.
6. H. H. Kieffer, J. M. Anderson, and K. J. Becker, "Radiometric calibration of spacecraft using small lunar images," *Proc. SPIE* **3870**, pp. 193–205, 1999.
7. H. H. Kieffer, T. C. Stone, R. A. Barnes, S. Bender, R. E. E. Jr., J. Mendenhall, and L. Ong, "On-orbit radiometric calibration over time and between spacecraft using the Moon," *Proc. SPIE* **4881**, pp. 287–298, 2003.
8. H. H. Kieffer, P. Jarecke, and J. Pearlman, "Initial lunar calibration observations by the EO-1 hyperion imaging spectrometer," *Proc. SPIE* **4480**, pp. 247–258, 2002.
9. F. Castelli and R. L. Kurucz, "Model atmospheres for vega," *Astron. Astrophys.* **281**, pp. 817–832, 1994.
10. D. S. Hayes, "Stellar absolute fluxes and energy distributions from 0.32 to 4.0 microns," in *Calibration of Fundamental Stellar Quantities, Proceedings of the Symposium, Como, Italy, May 24-29, 1984* D. Reidel Publishing Co., (Dordrecht), pp. 225–252, 1985.
11. D. W. Strecker, E. F. Erickson, and F. C. Witteborn, "Airborne stellar spectrometry from 1.2 to 5.5 microns - absolute calibration and spectra of stars earlier than M3," *Astrophys. J. Supp.* **41**, pp. 501–512, 1979.
12. K. Lumme and E. Bowell, "Radiative transfer in the surfaces of atmosphereless bodies. I. theory," *Astron. Jour.* **86**, pp. 1694–1704, 1981.
13. B. J. Buratti, J. K. Hillier, and M. Wang, "The lunar opposition surge: Observations by Clementine," *Icarus* **124**(2), pp. 490–499, 1996.
14. J. K. Hillier, "Shadow-hiding opposition surge for a two-layer surface," *Icarus* **72**, pp. 15–27, 1997.
15. P. Helfenstein, J. Veverka, and J. Hillier, "The lunar opposition effect: a test of alternative models," *Icarus* **128**, pp. 2–14, 1997.
16. J. Hillier, B. Buratti, and K. Hill, "Multispectral photometry of the Moon and absolute calibration of the clementine uv/vis camera," *Icarus* **141**, pp. 205–225, 1999.
17. Y. G. Shkuratov, M. A. Kreslavsky, A. A. Ovcharenko, D. G. Stankovich, E. S. Zubko, C. Pieters, and G. Arnold, "Opposition effect from clementine data and mechanisms of backscatter," *Icarus* **141**, pp. 132–155, 1999.
18. B. W. Hapke, *Theory of Reflectance Spectroscopy*, Cambridge University Press, Cambridge, 1993. 455 pp.
19. C. Wehrli, "Spectral solar irradiance data." World Climate Research Program (WCRP) Publication Series No. 7, WMO ITD-No. 149, 1986. pp. 119–126.
20. T. B. McCord and T. V. Johnson, "Lunar spectral reflectivity (.3 to 2.5 microns) and implications for remote mineralogical analysis," *Science* **169**, pp. 854–858, 1970.
21. A. P. Lane and W. M. Irvine, "Monochromatic phase curves and albedos for the lunar disk," *Astronom. J.* **78**, pp. 267–277, 1973.
22. T. B. McCord, R. N. Clark, B. R. Hawke, L. A. McFadden, P. D. Owensby, and C. M. Pieters, "Moon - near-infrared spectral reflectance, a first good look," *J. Geophys. Res.* **86**, pp. 10883–10892, Nov. 10 1981.
23. P. G. Lucey, B. R. Hawke, C. M. Pieters, J. W. Head, and T. B. McCord, "A compositional study of the Aristarchus region of the Moon using near-infrared spectroscopy," *Jour. Geophys. Res.* **91**, pp. D344–D354, 1986.
24. A. McEwen, E. Eliason, P. Lucey, E. Malaret, C. Pieters, M. Robinson, and T. Sucharski, "Summary of radiometric calibration and photometric normalization steps for the clementine uvvis images," *Lunar and Planetary Science* **29**, pp. 1466–1467, 1998.
25. A. S. McEwen, "A precise lunar photometric function," *Lunar and Planetary Science* **27**, pp. 841–842, 1996.